RESEARCH ARTICLE

Computer Tomography and Magnetic Resonance Image Manifestations of Primary Hepatic Neuroendocrine Cell Carcinomas

Juan Huang, Jian-Qun Yu*, Jia-Yu Sun

Abstract

Aim: This study aims to investigate the manifestation of CT, MRI and dynamic enhanced scans for primary hepatic neuroendocrine cell carcinoma. Methods: CT or MRI arterial and venous phase scan images of 19 cases of pathologically confirmed PHNEC were retrospectively analyzed. Results: 14 cases (73.68%) with single lesion, 5 cases (26.3%) with multiple lesions, with an average diameter of 13.2 cm. Some 12 cases (63.16%) showed inhomogeneous enhancement, seven cases (36.8%) showed homogeneous enhancement, 13 cases (68.4%) demonstrated significant enhancement in the arterial phase, 13 cases (68.4%) had significantly enhanced portal venous phase including 7 cases (36.8 %) with portal venous phase density or signal above the arterial phase and 5 cases (26.3%) with the portal vein density or signal below the arterial phase. Seven cases (36.8%) had continued strengthened separate shadows in the center of the lesion. Thrombosis were not seen in portal veins. Conclusion: CT and MRI images of liver cell neuroendocrine carcinoma have certain characteristics that can provide valuable information for diagnosis and differential diagnosis.

Keywords: Neuroendocrine cell carcinoma - liver - Tomography/X-ray compute - MRI

Asian Pac J Cancer Prev, **15 (6)**, 2759-2764

Introduction

Neuroendocrine carcinoma was also known as carcinoid or addicted silver cell carcinoma, often occurred in the gastrointestinal tract. The clinical hepatic neuroendocrine tumors mostly was induced by the transfer of intestines and pancreas and others (Pilichowska et al., 1999; Solcia et al., 2000; Modlin et al., 2008; Schwartz et al., 2008; Yao et al., 2008; Zeng et al., 2013) with the histopathologic performance of organ-like growth pattern, the tumor cells was argyrophilic, so they had specific positive performance in the detection of chromogranin A (CgA) and synaptophysin (Syn) of immunohistochemistry (Chang et al., 2007; Huang et al., 2010; Kim et al., 2011; Park et al., 2012). Primarily hepatic neuroendocrine carcinoma (PHNEC) was very rare, accounting for 1-5% of primary liver tumors, and 0.8%-4.0% of systemic neuroendocrine tumors (Pilichowska et al., 1999; Solcia et al., 2000; Yao et al., 2008; Huang et al., 2010). Both the clinical symptoms and imaging findings were not specific, resulting in difficult for preoperative diagnosis. Most previous studies reported in the literature were about individual case (Pilichowska et al., 1999; Tohyama et al., 2005; Yalav et al., 2010; Hamanaka et al., 2012), no reports were about the features of CT and MRI imaging for bulk cases with PHNEC (Bader et al., 2001; Ulusan et al., 2005; Rufini et al., 2006; Krohn et al., 2011; Baek et al., 2013; Li et al., 2013). In this study, data of 19 cases with complete preoperative imaging data were analyzed retrospectively, and surgical resection or biopsy of the primary hepatic neuroendocrine carcinoma were performed to explore the performance characteristics of CT and MRI imaging for PHNEC in order to improve the level of image diagnosis and differential diagnosis for PHNEC.

Materials and Methods

Subjects

19 cases from West China Hospital of Sichuan University during January, 2008 to May, 2013 pathologically confirmed to be primary liver neuroendocrine cell carcinoma by surgical resection or puncture biopsy were collected, including 11 cases detected by preoperative CT scan and enhanced dual-phase scanning and 8 cases by dynamic contrast-enhanced MRI scans. 11 cases were males and 8 cases were females, aged from 7 to 72 years old with the average age of 47.15 years old. 6 cases of 19 cases had the first symptom of the right hypochondrium pain discomfort, 5 cases with no obvious physical symptoms including 3 cases of weight loss and cases of vomiting, 1 case of diarrhea and 1 case of stomach ulcer were accidentally found by B ultrosounic inspection. 16 cases had no history of hepatitis with negative hepatitis B virus by quantitative detection, 3 cases was hepatitis B

*Department of Radiology, West China Hospital, Sichuan University, Chengdu, Sichuan, China *For correspondence: jianqunyucn@163.com*

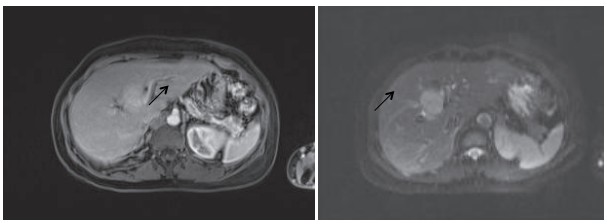

Figure 1. Hilar Physical Footprint was Found in 47-year-old woman by B untrasounic Inspection and MRI Enhanced Scan. A: homogeneous enhancement mass shadow in hilar arterial phase (black arrow). B: portal venous phase lesions continued to strengthen, the signal strength was more obvious than that of the arterial phase (black arrow)

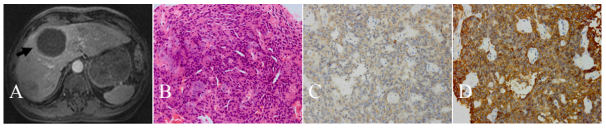

Figure 2. Upper Abdominal Discomfort in 71 Year-old Male. A: MRI enhanced scan: multiple lesions in the liver parenchyma, the largest lesions located in the left lobe of the liver inside and the right lobe anterior segment (black arrow), significantly liquefied necrotic in lesion center, enhancement edge portion in enhanced scan of the lesion. B: tumor cells arranged in trabecular or aciniform in HE staining (400×), nucleus centered, size was relatively consistent, some nuclei were mild atypia. C: Immunohistochemistry: CgA (+) (400×). D: SYN (+) (400×), with typical daisy group structure in neuroendocrine tumors

virus carrier with negative tumor markers AFP, CA19-9 and CA-125, 13 cases of normal liver function and 6 cases of abnormal liver function. This study was conducted in accordance with the declaration of Helsinki. This study was conducted with approval from the Ethics Committee of West China Hospital Sichuan University. Written informed consent was obtained from all participants.

Inspection techniques and parameters

11 patients in this set of cases in the study were inspected with 64-slice spiral CT scanner (Philips Brilliance, Holland), patients was fasting more than 8 h before the test, drank 500~1000 ml warm water for 10 minutes before the scan. Conventional supine for plain scan and enhanced dual-phase scanning. Plan scanning parameters: 120 kV, 90 mA, spiral, collimator with size of 64 mm×0.625 mm, bed speed of 12 mm/s and 7 for pitch. Contrast agent was Ultravist (ultravist, 300 mgI/ml, Bayer Schering Pharma, Berlin Germany), injected 80ml by forearm intravenous bolus with high-pressure injector (Medrad, USA), the injection flow rate was 2.5 ml/s, performed arterial, venous phase scan 25s and 50s after the beginning of injection.

5 patients were detected using 1.5T MRI (Sonata; Siemens, Germany) scanners, 3 cases using 3.0T MRI (Trio; Siemens, Germany) scanner. Phased array body diaphragm coil was used with the level scan range from the top to the level of the lower edge of the liver. Firstly, the abdominal scan was routinely performed with imaging sequences and parameters as follows: horizontal plane T2WI (TR1000 ms, 83 ms TE, 8 mm slice thickness, 9.2 mm layer from) and T1WI (TR100 ms, 4.8 ms TE, 8 mm slice thickness, 9.2 mm layer from). 3D2VIBE sequence was used for three dynamic enhanced MRI with imaging parameters of 4.2 ms TR, 1.8 ms TE, 2.0 mm thickness and 12 ° excitation angle. Contrast agent was Gd-DTPA (Magnevist; Bayer Schering Germany) with a dose of 0.2 mmol/kg and injection flow rate of 2.5 ml/s injected via cubital vein using a high-pressure syringe. Three phase enhanced scan was performed 15 s, 40 s and 65s after contrast injection. Finally T1WI axial scanning was performed to get the image of the balance phase, the imaging parameters was 124 ms TR, 2.5 ms TE, 8 mm slice thickness and 9.2 mm layer.

Image evaluation

The images were read by the two physicians using blind method (unknown about surgical pathology results). According to the results of CT, MRI scan and enhanced dual-phase scanning, the number of lesions, location, size, shape, presence and with or without necrotic lesions, hemorrhage, calcification, enhancement features of the lesion in arterial and portal venous phase, the relationship between vascular lesions in liver and bile duct, portal vein tumor thrombus formed or not, with or without local or distant lymph node metastasis were recorded. Came to a consensus if disagreements through discussion.

General forms were divided into three types: round or oval, lobulated and irregular shape. Size: taking images in the portal venous phase as standards, single lesion was measured as the maximum diameter of the lesions, multiple lesions were measured as the maximum diameter of the largest lesion. Lesions strengthening: significantly enhanced and mild enhancement (taking the change of same interest area to the most obvious strengthen area (10 mm^2) for judging prospective, CT slightly enhanced represented CT value increase <30 HU, significantly enhanced indicated CT value ≥30 HU, MRI was judged by the signal strength for the interest area before and after T1 W plain and enhanced scans increase or not). Enhancement patterns were divided into homogeneous enhancement and heterogeneous enhancement, multiple lesions were determined by the enhancement pattern of the majority lesions.

Results

Mass number, shape, size, and occurrence sites

Of the 19 patients, 14 cases (14/19, 73.68%) showed the liver parenchyma single lesion (Figure 1), 5 cases (5/19, 26.32%) showed multiple lesions in the liver parenchyma (Figure 2), one case with splenic metastasis, one case with multiple pulmonary metastases, and one case with liver lesion invading adjacent gallbladder. 8 cases with left hepatic lobe (8/19, 42.11%) lesion, 6 cases with the right lobe (6/19, 31.58%), five cases with common involvement of the inside of the left hepatic lobe and the right lobe (5/19, 26.32%). The maximum diameter of the lesion was 2.5~22.5 cm with the average size of 13.2 cm. 11 cases (11/19, 57.89%) lesions were round or oval shape, 5 cases of (5/19, 26.32%) lobulated, 3 cases (3/19, 15.79%) were irregular.

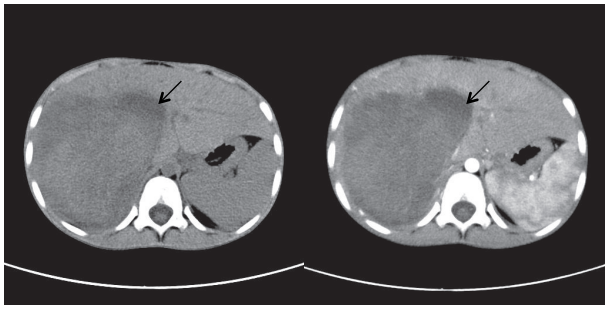

Figure 3. Enhanced CT Scan of 6 Years Old Males. A: plain scan cystic mass in the right lobe, the center had obvious liquefaction necrosis and hemorrhage sheet with high density (black arrow). B: significant continued enhancement in enhanced arterial phase (black arrow)

CT

In the lesions of the 11 cases, four cases showed little uniform density with low-density mass by plain scan (4/11, 36.36%), four cases (4 /11, 36.36%) had liquefaction necrosis in lesions, 3 cases (3/11, 27.27%) showed a cystic mass including 2 cases (2/11, 18.18%) of the sheet of high density hemorrhage (Figure 3), no calcification was seen in all lesions (0/11, 0%). Seven cases in artery phase (7/11, 63.63%) showed tumor parenchyma heterogeneous enhancement (Figure 4), and 4 cases (4/11, 36.36%) showed homogeneous enhancement. 8 cases (8/11, 72.72%) was significantly enhanced, 3 cases (3/11, 27.27%) with mild enhancement. 7 cases in portal venous phase (7/11, 63.63%) was significantly enhanced tumor parenchyma, 4 cases (4/11, 36.36%) with mild enhancement. 5 patients (5/11, 45.45%) showed higher density in portal venous phase than that in the arterial phase (Figure 4), 2 cases (2/11, 18.18%) with lower density in portal venous phase than that of the arterial period, two cases (2/11, 18.18%) showed significantly enhanced performance both in arterial and portal venous phases with the same degree of enhancement, 1 case (1/11, 9.09%) was slightly enhanced both in arterial and portal venous phases (Figure 3). Continued strengthen separate shadow was seen in the center of the in 4 cases in portal venous phase (4/11, 36.36%) (Figure 4). No tumor thrombus of the portal vein was observed in all cases. 3 cases (3/11, 27.27%) lesions oppressed common hepatic duct and bile duct, remote intrahepatic bile duct was dilatation. 1 case (1/11, 9.09%) had lesions invading adjacent gallbladder. 2 cases (2/11, 18.18%) appeared lymph nodes next to the abdomen.

MRI

In eight case MRI scans, 3 cases (3/8, 37.50%) showed lower T1W signal lesions with clear edge and slightly higher T2W signal, five cases (5/8, 62.50%) with inhomogeneous mixed T1W and T2W signal lesions with liquefaction necrosis in the center. 5 cases (5/8, 62.5%) showed inhomogeneous parenchyma enhancement lesions Figure 5), 3 cases (3/8, 37.5%) showed homogeneous enhancement (Figure 1), 5 cases (5/8, 62.50%) was significantly enhanced in dynamic contrast-enhanced of arterial phase (Figure 6), 3 cases (3/8, 37.5%) was slightly enhanced. 6 cases (6/8, 75.0%) showed significantly enhanced tumor parenchyma lesions in portal venous

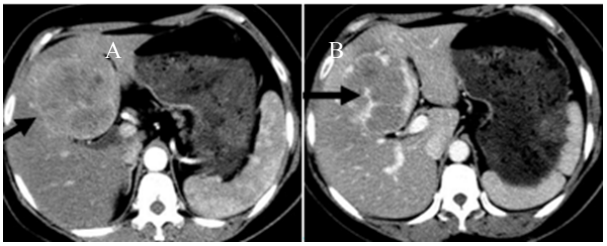

Figure 4. CT Enhanced Scan of 41 Years Old Women, Medial Mass in the Left Hepatic Lobe Segment. A: Mild enhancement in tumor parenchyma (black arrow). B: Sustained significant enhancement portal vein lesions, within which sustained separated shadow was seen (black arrow), enhancement in the portal vein was more obvious than the arterial phase enhancement

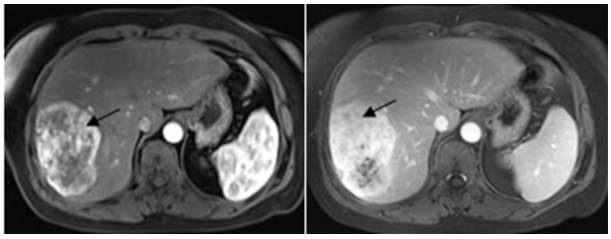

Figure 5. Enhanced MRI Scans in 52 Year-old Man, Medial Segment Mass in the Left Lobe of the Liver. A: Arterial lesions showed ring enhancement (black arrow). B: Continuous ring enhancement shadow of portal vein tumor (black arrow), arterial phase signal was higher than that of the portal venous phase with enhanced separate shadows

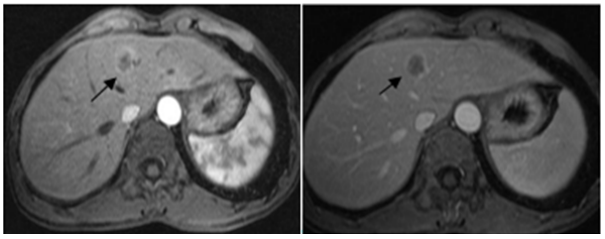

Figure 6. Enhanced MRI Scans for 41 Years Old Female, Mass in the Right Lobe. A: Obviously enhancement tumor parenchyma (black arrow). B: Continued enhancement of the portal vein lesions (black arrow), portal venous phase signal was higher than the arterial phase signal

phase (Figure 6), two cases (2/8, 25.0%) was slightly enhanced. 3 cases (3/8, 37.5%) showed higher signal in portal venous phase than that of the arterial phase (Figure 6), 2 cases (2/8, 25.0%) showed lower signal in portal venous phase than that of the arterial phase (Figure 5), 3 cases (3/8, 37.50%) had similar signal between the arterial and portal venous phase, three cases (3/8, 37.50%) had continued strengthening separated shadow in the center of lesions (Figure 6). One case had liver lesions simultaneously companied with low signal stone shadow within the common bile duct. No tumor thrombus was seen in all portal veins of the cases.

Surgical pathology

5 cases were diagnosed by puncture, 14 cases were performed surgical resection. The removed tumor had sharp edges and medium texture. 3 cases had tumor capsule with fish-shaped cross section. Tumor was

composed of many small cell nests, cell strings or large cell clumps under light microscope. Eosinophilic granules were seen in cytoplasm, nucleus was round and centered, the nuclear membrane was thin, capillary network was rich. Immunohistochemical examination: 15 cases had positive cell neuroendocrine markers CgA (+), 14 cases had Syn (+), all AFP labeled specimens of the 10 cases showed negative.

Discussion

PHNEC was one of carcinoid tumors, also known as argyrophil cell tumor. Less domestic and foreign reports on PHNEC was available, as well as little understanding of its origin (Pilichowska et al., 1999; Solcia et al., 2000; Yao et al., 2008), three assumptions were proposed currently: 1) tumor cells derived from intrahepatic biliary epithelial neuroendocrine cells. 2) tumor tissue derived from the liver ectopic pancreas or adrenal tissues. 3) tumor cells derived from the liver pluripotent stem cells. Neuroendocrine cell carcinoma often occurred from the bronchi, gastrointestinal tract, pancreas and other parts, occasionally was seen in the prostate, retroperitoneal, gall bladder, uterus, etc. (Pilichowska et al., 1999; Modlin et al., 2008; Yao et al., 2008; Zeng et al., 2013). Liver neuroendocrine carcinoma found in clinical mostly induced by the intestines and pancreas transfer, PHNEC was very rare originating in the liver (Pilichowska et al., 1999; Tohyama et al., 2005; Hamanaka et al., 2012; Yalav et al., 2012), accounting for 1%-5% of all liver cancer, and 0.8% -4.0% of systemic neuroendocrine tumors, the imaging findings were lack of specificity, leading to difficultly preoperative diagnosis (Pilichowska et al., 1999; Bader et al., 2001; Tohyama et al., 2005; Ulusan et al., 2005; Krohn et al., 2011; Yalav et al., 2012; Baek et al., 2013). Patients generally did not have carcinoid syndrome and were lack of specific clinical symptoms and signs. They may have no symptoms when early tumor was small, they had symptoms such as upper abdominal discomfort, loss of appetite, fatigue and weight loss when the tumor increased, so the tumors often were larger when being diagnosed (Pilichowska et al., 1999; Tohyama et al., 2005; Ulusan et al., 2005). In the 19 cases of this group, 6 cases showed right hypochondrium pain discomfort, 5 cases with no obvious physical symptoms including 3 cases of weight loss, 2 cases of vomiting, 1 case of diarrhea and 1 case of stomach ulcer accidentally found by B ultrosounic inspection, one case went for treatment due to gastric ulcer and one case due to diarrhea. 16 patients had hepatitis B virus quantitatively detected to be negative, 3 cases were hepatitis B virus carrier, the tumor markers AFP, CEA, CA19-9 and CA-125 were negative. 13 cases had normal liver function, 6 cases with abnormal liver function. Clinical manifestations were consistent with the literature (Pilichowska et al., 1999; Modlin et al., 2008; Schwartz et al., 2008). The maximum diameter of the lesions for 19 cases with PHNEC was 2.5~22.5 cm and the average size of 13.2 cm, only two cases had lesion diameters were less than 3 cm, 9 cases with diameters greater than 10 cm, 3 cases with diameters greater than 20 cm. 73.68% (14/19) showed a single lesion, 26.32% (5/19) showed multiple lesions. 42.11% (8/19) located in the left lobe, 31.58% (6/19) in the right lobe, 26.32% (5/19) patients with left hepatic lobe and right lobe segments simultaneously involved, their distribution was consistent with reported literature (Pilichowska et al., 1999; Chang et al., 2007; Schwartz et al., 2008).

Kim et al. (2011) analyzed the helical CT results of 38 cases with liver cell neuroendocrine carcinoma and divided enhancement into three categories: 1) carcinoid hepatocellular carcinoma types with obvious arterial phase enhancement, enhancement was delayed in portal venous phase. 2) Carcinoid cholangiocarcinoma type with no enhancement in the arterial phase, enhancement was delayed in portal venous phase. 3) Mixed type with heterogeneous enhancement in arterial phase, continue strengthen in the portal venous phase. However, in the analyzed 38 cases, only 3 cases were original PHNEC, 24 cases were metastatic liver neuroendocrine cell carcinoma, and 11 cases can not be judged as primary or metastatic cancers. Its imaging findings could not represent the PHNEC performance. In 19 cases of this group, 17 cases found lesions only in liver, one case of splenic metastasis and one case of multiple pulmonary metastases confirmed by pathology. No tumors in other organs were detected in the radiological and clinical performance of the remaining cases. The CT and MRI scan and enhanced scan results of 19 cases with PHNEC in arterial and portal venous phases had varying degree of enhancement, 13 cases (68.42%) had arterial phase enhancement, 13 cases (68.42%) was significantly enhanced in portal venous phase, of which 7 cases (5 cases by CT and 2 cases by MRI), accounting for 63.84%. The signal or density of the portal venous lesions was higher than that of the arterial phase, which was similar to enhancement type of classified bile duct cell type in liver cancer of Kim' rerport. 5 cases (2 cases of CT and 3 cases of MRI) accounted for 26.32%, the density or signal of portal vein was lower than that of arterial lesions, which was similar to enhancement type of classified liver cancer type in liver cancer of Kim' rerport. Combined with its pathological features, we believed that the significantly enhanced primary liver cancer cell neuroendocrine tumor center was related with the rich capillary network. Li et al. (2013) analyzed the enhanced MRI scans and diffusion-weighted scans (DWI) images of 8 patients with PHNEC and considered that typical performance of PHNEC was larger tumor and hypervascular tumor often accompanied by satellite lesions, and the arterial phase significantly enhanced and portal rapid washout, amicula like enhancement was seen in the balance phase, restricted diffusion on DWI images. Similar to the report, the majority of 19 PHNEC cases also showed hypervascular tumors, but demonstrated a variety of ways, 5 cases showed significantly enhanced arterial, portal venous rapid washout, 7 cases showed sustained arterial and portal venous enhancement. We believed that the enhanced way and the tumor vascular network within the tumor were related with the balance of fibrosis. 7 cases in 19 patients (36.84%) had sustained enhanced separated shadow in the center of the lesions, which was more characteristic signs. Analyzing that this was related with slower growth rate and central liquefaction necrosis

insufficiency.

Primary liver cell neuroendocrine carcinoma was a rare primary liver cancer, the imaging performance was still lack of awareness and understanding, resulting in often misdiagnosis (Bader et al., 2001; Ulusan et al., 2005; Rufini et al., 2006; Krohn et al., 2011; Baek et al., 2013; Li et al., 2013). The main differential diagnosis was primary hepatocellular carcinoma and bile duct carcinoma (Kim et al., 2011; Yalav et al., 2012; Li et al., 2013). All CT and MRI of 19 cases was preoperatively diagnosed. 7 cases were misdiagnosed as bile duct carcinoma, 5 cases as hepatocellular carcinoma, 1 6-year-olds child with huge cystic liver tumor was (Figure 6) misdiagnosed as parasitic infections, 6 cases had undetermined nature of the lesion. Both PHNEC and cholangiocarcinoma can be expressed as continuous heterogeneous enhancement of the portal vein, especially difficult to identify when larger tumor compressed the adjacent bile duct, intrahepatic bile duct dilatation occurred around the lesions. The key differential point was that PHNEC was hypervascular tumors, appeared strengthen and larger lesions even in the early arterial period, the centersten accompanied by liquefaction necrosis. Strengthening separated shadow was visible portal venous phase, while bile duct carcinoma had not so rich blood supply and obvious enhanced arterial phase with often delayed enhancement. The difficulty of identification for primary hepatocellular carcinoma and neuroendocrine liver cancer was that both can be manifested as arterial phase enhancement. Primarily hepatocellular carcinoma patients usually had a history of hepatitis and cirrhosis, alpha-fetoprotein (AFP) rises, CT and enhanced MRI scan showed "fast in and out", significantly enhanced arterial lesions, portal venous phase decreased rapidly to low density. Tumor often accompanied by metastasis and intrahepatic portal vein thrombus tumor. While the neuroendocrine liver carcinoma was different, which rarely associated with a history of hepatitis and cirrhosis, often without increased AFP. 19 patients had no elevated AFP, and no case had portal vein thrombosis. The diagnosis of neuroendocrine cell carcinoma ultimately depended on the pathological diagnosis, immunohistochemistry, electron microscopy techniques and others (Pilichowska et al., 1999; Ulusan et al., 2005; Chang et al., 2007; Yao et al., 2008). Chromgranin (CgA) and synaptophysin (Syn) in immunohistochemistry were detected to be positive, especially typical daisy group structure of the neuroendocrine tumors was an important basis for diagnosis of the disease (Pilichowska et al., 1999; Schwartz et al., 2008). 15 patients had positive CgA (+), 14 cases with positive Syn (+). Comprehensive inspection was performed at the same time. A total of 122 patients with gastroenteropancreatic neuroendocrine neoplasm were analyzed retrospectively (Zeng et al., 2013), and the results showed that 32 patients showed distant metastases, of which 29 cases (90.7%)had liver metastasis. It is necessary to perform the physical examination in the diagnosis of primary hepatic neuroendocrine cell carcinoma.Exception of extrahepatic primary lesions, especially the primary lesion of pancreas and intestinal tract , it is also helpful that postoperative clinical follow-up and auxiliary examination to discover potential primary lesionsl.

In conclusion, CT and MRI scan enhancement of PHNEC showed a certain characteristics, the typical manifestations of tumor was large, apparent enhancement appeared in the enhanced scan of the arterial and portal venous phase, continued strengthen separated shadows often appeared in the center of the lesions, and no thrombosis in the portal vein, if the clinical history was longer at the same time, with no history of hepatitis and cirrhosis, normal AFP levels, it should take PHNEC into account. Dynamic contrast-enhanced CT and MRI scans can provide valuable information for the diagnosis and differential diagnosis of hepatic neuroendocrine cell carcinoma before surgery.

References

Bader TR, Semelka RC, Chiu VC, Armao DM, Woosley JT (2001). MRI of carcinoid tumors: spectrum of appearances in the gastrointestinal tract and liver. *J Magn Reson Imaging*, **14**, 261-9.

Baek SH, Yoon JH, Kim KW (2013). Primary hepatic neuroendocrine tumor: gadoxetic acid (Gd-EOB-DTPA)-enhanced magnetic resonance imaging. *Acta Radiol*, **2**, 2-6.

Chang S, Choi D, Lee SJ, et al (2007). Neuroendocrine neoplasms of the gastrointestinal tract: classification, pathologic basis, and imaging features. *Radiographics*, **27**, 1667-79

Hamanaka M, Nakahira S, Takeda Y, et al (2012). A case of primary neuroendocrine carcinoma of the bile duct. *Gan To Kagaku Ryoho*, **39**, 2125-7.

Huang YQ, Xu F, Yang JM, Huang B (2010). Primary hepatic neuroendocrine carcinoma: clinical analysis of 11 cases. *Hepatobiliary Pancreat Dis Int*, **9**, 44-8.

Kim JE, Lee WJ, Kim SH, et al (2011). Three-phase helical computed tomographic findings of hepatic neuroendocrine tumors: pathologic correlation with revised WHO classification. *J Comput Assist Tomogr*, **35**, 697-702.

Krohn M, Grieser C, Weichert W, Pascher A, Denecke T (2011). Well-differentiated neuroendocrine carcinoma mimicking an echinococcus cyst ofthe liver in CT-MRI findings with hepatocyte specific contrast material. *J Gastrointestin Liver Dis*, **20**, 439-42.

Li RK, Zhao J, Rao SX, et al (2013). Primary hepatic neuroendocrine carcinoma: MR imaging findings including preliminary observation on diffusion-weighted imaging. *Abdom Imaging*, **38**, 1269-76.

Modlin IM, Oberg K, Chung DC, et al (2008). Gastroenteropancreatic neuroendocrine tumours. *Lancet Oncol*, **9**, 61-72.

Park CH, Chung JW, Jang SJ, et al (2012). Clinical features and outcomes of primary hepatic neuroendocrine carcinomas. *J Gastroenterol Hepatol*, **27**, 1306-11

Pilichowska M, Kimura N, Ouchi A, et al (1999). Primary hepatic carcinoid and neuroendocrine carcinoma: clinicopathological and immunohistochemical study of five cases. *Pathol Int*, **49**, 318-24.

Rufini V, Calcagni ML, Baum PR (2006). Imaging of neuroendocrine tumors. *Sem Nucl Med*, **36**, 228-47.

Schwartz G, Colanta A, Gaetz H, Olichney J, Attiyeh F (2008). Primary carcinoid tumors of the liver. *World J Surg Oncol*, **6**, 91.

Solcia E, Kloppel G, Sobin LH (2000). WHO histologic typing of endocrine tumours. 2nd ed. Springer: Berlin.

Tohyama T, Matsui K, Kitagawa K (2005). Primary hepatic carcinoid tumor with carcinoid syndrome and carcinoid heart disease: A case report of a patient on long-term follow-up.

Intern Med, **44**, 958-62.
Ulusan S, Kizilkilic O, Yildirim T, et al (2005). Primary hepatic carcinoid tumor: dynamic CT findings. *Abdom Imaging*, **30**, 281-5.
Yalav O, Ülkü A, Akçam TA, Demiryürek H, Doran F (2012). Primary hepatic neuroendocrine tumor: Five cases with different preoperative diagnoses. *Turk J Gastroenterol*, **23**, 272-8.
Yao JC, Hassan M, Phan A, et al (2008). One hundred years after "carcinoid": epidemiology of and prognostic factors for neuroendocrine tumors in 35, 825 cases in the United States. *J Clin Oncol*, **26**, 3063-72.
Zeng YJ, Liu L, Wu H, et al (2013). Clinicopathological features and prognosis of gastroenteropancreatic neuroendocrine tumors: analysis from a single-institution. *Asian Pac J Cancer Prev*, **14**, 5775-81.